

The studies [1-6] examined the settling of gas suspensions in an enclosed volume, a process which is of interest in a wide range of production operations. The authors of [1-3] studied hindered steady-state settling in a unidimensional approximation in order to establish the dependence of the settling rate on particle concentration. A two-velocity model was used in [4], again in the unidimensional case, for highly concentrated suspensions in order to find the nonsteady rate of particle deposition. Analysis of the settling of a suspension in a two-dimensional formulation within the framework of the two-velocity model [5, 6] showed that the non-unidimensional flows of liquid which develop significantly alter the characteristics of unidimensional settling.

Below, we use the methods of the mechanics of multiphase media [7] to study the settling of a gas suspension in a closed vessel. It is shown that allowing for the compressibility of the gas leads to the occurrence of gasdynamic oscillations of the carrier phase which, under certain conditions, have a significant effect on particle deposition. In particular, these oscillations intensify the settling of the suspension.

1. Formulation of the Problem. Let a gas suspension consisting of solid spherical monodisperse particles and a perfect gas be located in a closed vessel at the initial moment of time. The particles are uniformly distributed over the volume of the vessel. Under the influence of gravity, the particles begin to fall, and, as a result of friction, this falling leads to motion of the gas. The problem is to calculate the induced motion of the dispersion medium up to the point of complete deposition of the particles. It is assumed that the dimensions of the vessel are greater in one of the horizontal directions than in the other. This allows us to examine a two-dimensional problem (the cross section of the vessel being a square). The volume fraction of particles is negligibly small, and collisions between the particles are not considered. It is assumed that the gas and the particles have the same temperature (one-temperature medium), which at the initial moment of time is equal to T_0 .

With allowance for the above assumptions, we can write the equations of motion of the viscous, heat-conducting gas as follows in dimensionless variables

$$\frac{\partial \rho_1}{\partial t} + \nabla(\rho_1 \mathbf{U}_1) = 0, \quad p = \rho_1 T; \quad (1.1)$$

$$\frac{\partial \mathbf{U}_1}{\partial t} + (\mathbf{U}_1 \nabla) \mathbf{U}_1 = -\frac{1}{\gamma M^2 \rho_1} \nabla p + Fr \mathbf{G} + \frac{1}{Re \rho_1} \left(\nabla \mathbf{U}_1 + \frac{1}{3} \nabla (\nabla \mathbf{U}_1) \right) - \mathbf{F}; \quad (1.2)$$

$$\rho_1 \frac{d_1 T}{dt} + \gamma_1 \rho_2 \frac{d_2 T}{dt} = -(\gamma - 1) p (\nabla \mathbf{U}_1) + \frac{\gamma}{Re Pr} \Delta T \quad \left(\frac{d_i}{dt} = \frac{\partial}{\partial t} + \mathbf{U}_i \nabla \right), \quad (1.3)$$

$$\Delta = \frac{\partial^2}{\partial x^2} + \frac{\partial^2}{\partial y^2}, \quad \mathbf{U}_1 = (u_1, v_1), \quad \mathbf{G} = (0, -1), \quad M^2 = \frac{w^2}{\gamma R T_0},$$

$$\gamma_1 = \frac{c_V}{c_2}, \quad Fr = \frac{gL}{w^2}, \quad Re = \frac{wL\rho_{10}}{\eta}, \quad Pr = \frac{\eta c_p}{\lambda}.$$

Here, t is time; x and y are cartesian coordinates (the x axis is directed along the lower boundary of the region, while the y axis is perpendicular to it); $\rho_1, \mathbf{U}_1, p, T$ are the density, velocity, pressure, and temperature of the gas; \mathbf{G} is the vector of the gravitational force; \mathbf{F} is the phase interaction force; ρ_2 is the mean density of the disperse phase; M, Fr, Re, Pr are the Mach, Froude, Reynolds, and Prandtl numbers; γ is the adiabatic exponent of the gas; γ_1 is the ratio of the heat capacity of the gas at constant volume c_V to the heat capacity of the particles c_2 ; $w = \rho_2^0 d^2 g / 18\eta$ is the steady-state rate of fall of a single

particle calculated in the Stokes approximation; ρ_2^0 and d are the true density and diameter of the particles; g is acceleration due to gravity; η is the absolute viscosity of the gas; R is the gas constant; L is the side of the region; ρ_{10} is the density of the gas near the bottom surface at the initial moment of time; c_p is the heat capacity of the gas at constant pressure; λ is the thermal conductivity of the gas. As the characteristic scales of length, velocity, time, density, temperature, and pressure, we respectively took L , w , L/w , ρ_{10} , T_0 , $R\rho_{10}T_0$. Viscous dissipation of energy was ignored.

We assumed that the change in the momenta of the phases during their interaction was determined by the frictional force

$$F = Fr \frac{Re_p}{24} c_d(Re_p) \frac{\rho_2}{\rho_1} (U_1 - U_2), \quad (1.4)$$

where U_2 is the velocity of the disperse phase; Re_p is the instantaneous Reynolds number of a particle; $c_d(Re_p)$ is the drag coefficient of the particles.

We will use the approach proposed in [8] to describe the motion of the disperse phase. At the initial moment of time, the entire region being examined is hypothetically subdivided into a finite set of identical subregions. The motion of all particles which happen to fall within an arbitrary subregion is described by introducing a so-called macroparticle in place of individual particles. The mass of each macroparticle is equal to the sum of the mass of the physical particles which comprise it. The drag force is equal to the sum of the drag forces of the physical particles associated with the given macroparticle. The subdivision is done so that the masses of all of the macroparticles are the same. Thus, the mass of one macroparticle is equal to the ratio of the total mass of the disperse phase in the region to the number of macroparticles.

The motion of the k -th macroparticle is regarded as the motion of a material point and is described (in dimensionless form) by the equations

$$\frac{dU_k}{dt} = FrG + Fr \frac{Re_p}{24} c_d(Re_p) (U_1 - U_k), \quad \frac{dr_k}{dt} = U_k \quad (1.5)$$

(U_k and r_k are the velocity and radius-vector of the k -th macroparticle).

The condition of "adhesion" is imposed at the boundary of the region and the initial temperature is maintained ($U_1 = 0$, $T = 1$). The particle collisions with the bottom walls are assumed to be perfectly inelastic, while the collisions with the other walls are assumed to be perfectly elastic. At the initial moment of time, the gas is in static equilibrium. The particles are at rest and are distributed uniformly over the volume: $U_1 = U_2 = 0$, $\rho_1 = \exp(-\gamma M^2 Fr \gamma)$, $\rho_2 = M_{21}$, $T = 1$ ($M_{21} = \rho_2^0 n_0 \pi d^3 / 6 \rho_{10}$ is the ratio of the initial mass fractions of the phases and n_0 is the initial particle concentration). Below, we study the settling of particles small enough so that the Stokes formula $c_d = 24/Re_p$ is valid for the drag coefficient.

The process being examined is actually isothermal, since the temperature gradients caused by pressure forces are extremely small. The use of energy equation (1.3) instead of isothermality condition $T = \text{const}$ was due to the need to adequately describe the acoustic effects, which play an important role here (the isothermality condition would have led to an isothermal sonic velocity in the system and, thus, to distortion of the actual pattern of the process).

2. Numerical Method. System (1.1)-(1.3), describing the flow of the gas, was solved numerically on a uniform grid by the finite-difference method of coordinate splitting [9]. The system of equations of motion of the particles (1.5) was integrated numerically by Euler's method.

The values of gas velocity at the points where the macroparticles were located were found by linear interpolation, while the values of the velocity and mean density of the disperse phase at the grid nodes were found by averaging the parameters of the macroparticles closest to each node. A detailed description of the numerical method is given in [8].

The calculations were performed on a 21×21 grid. Here, 1600 macroparticles were introduced into the region. The time step of the integration corresponded to a Curant number of 0.5. Control calculations showed that the numerical solution obtained does not depend on the grid parameters or the number of macroparticles. In all of the calculations, $Pr = 1$, while the remaining parameters were varied.

3. Basic Laws of the Process. Gravity causes the particles to begin to fall, with the particles entraining the gas as they descend. During the time $t < t_*$, the gas placed in motion does not "feel" the bottom wall of the vessel, and its elastic properties are not manifest; $t_* \sim t_s$, where t_s is the characteristic acoustic time (the time over which the sound wave travels a distance equal to the height of the region; $t_s = M$ when the method of obtaining dimensionless parameters we employed is used). It is during the time t_* that a high-pressure region is formed near the bottom surface. This region initially slows and subsequently reverses the gas flow. During the time $t < t_*$, the gas entrained by the particles is accelerated and, in turn, increases the rate of fall of the particles. This self-accelerating process is similar to the processes which take place when a collection of particles falls in an infinite medium [10].

At $t > t_*$, the settling process differs qualitatively from that studied in [10]. The compression wave that is formed is reflected from the bottom wall and begins to propagate upward, slowing the descent of the particles. It moves downward after being reflected from the top wall of the vessel, and so forth. Decaying oscillations of the gas (a standing wave) are generated. These oscillations have an effect on particle deposition and, in turn, are affected by the latter process. The friction of the gas against the side walls leads to the formation of boundary layers and makes the deposition process non-unidimensional.

The pattern of the process is illustrated in Figs. 1 and 2. Curve 1 in Fig. 1 shows the time dependence of the vertical momentum of the gas $J = \int_0^1 \int_0^1 \rho_1 v_1 dx dy$, while curve 2 shows the time dependence of the vertical coordinate of the center of gravity of unsettled particles y_c for the parameters $Re = 30$, $M^2 = 0.05$, $M_{21} = 0.5$, $Fr = 40$. For the same parameters, Fig. 2 shows lines of particles connecting those macroparticles initially located at the horizontal levels $y = 1; 0.75; 0.5; 0.25$ (lines 1-4). Also shown are the velocity fields of the gas at the successive moments of time $t_1 = 0.13; 0.23; 0.48$ (a-c). In the given case, curve 1 coincides with the upper edge of the settling gas suspension. Due to the symmetry of the solution relative to the plane $x = 0.5$, in Fig. 2 we show only the left half of the region. The moments t_1, t_2 , and t_3 are indicated in Fig. 1. For the conditions being examined, the characteristic particle relaxation time, $t_r = 1/Fr = 0.025$, is an order less than the characteristic acoustic time $t_s = 0.22$.

It is evident from Fig. 1 that a self-accelerating regime of particle fall is realized at $t < t_* = 0.11$. At the moment $t_* = 0.13$, the maximum velocity of the gas reaches 3.3, while maximum particle velocity reaches 3.5, i.e., the rate of particle fall is 3.5 times greater than the rate for a single particle. Figure 2 illustrates the nonuniformity of the velocity field of the gas and the associated curvature of the particle lines - the particles fall more slowly near the side walls. At $t \geq t_*$, the gas begins to be slowed and reversed by the bottom wall (Fig. 2b). At the moment $t = 0.24$, the vertical momentum of the gas is equal to zero. The gas as a whole then begins to move upward. Since the time of velocity relaxation of the particles in this case is considerably shorter than the period of oscillation of the gas, their velocities quickly decrease and even change sign at this stage. Thus, the center of gravity of the entire collection of particles is lowered to a certain extent (curve 2 in Fig. 1). Since the velocity of the gas is maximal in the plane $x = 0.5$, the lines of the macroparticles ascend at this location (Fig. 2c), so that the upper boundary of the settling gas suspension becomes severely curved. After reversal near the top wall, the gas descends. Here, the rate of fall of the particles again increases. By the moment $t = 1.09$, complete settling has occurred and the amplitude of the gas oscillations has decreased by a factor of 30 compared to the initial amplitude.

Below, we analyze the effect of different parameters on the course of the process. The inverse of Fr is the dimensionless time of velocity relaxation of the phases. A decrease in Fr is accompanied by an increase in particle relaxation time, which slows the rate of momentum transfer from one phase to the other. It is for this reason that deposition becomes more uniform with a decrease in Fr . Thus, with the parameters in Fig. 1 but for $Fr = 10$, the momentum of the gas $J(t)$ at the moment of time $t = t_*$ decreases nearly by a factor of two. Meanwhile, the relation $y_c(t)$ is almost a straight line, since the particles do not "have time" to respond to the high-frequency oscillations of the gas.

A reduction in M is equivalent to an increase in sonic velocity in the gas, i.e., a reduction in the characteristic acoustic time and the associated duration of the first

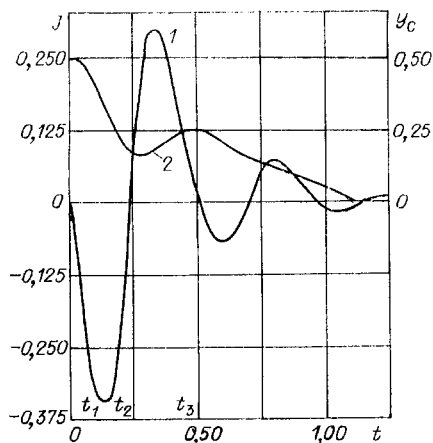


Fig. 1

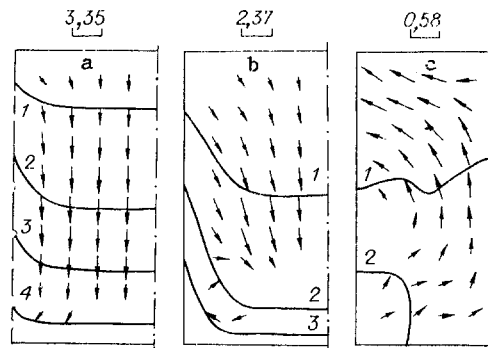


Fig. 2

(accelerated) stage of deposition. Accordingly, there is also a reduction in the initial amplitude of the gas oscillations and their effect on particle settling. If the particles are sufficiently inert, then they will not "sense" small gas oscillations which develop. Thus, at $M^2 = 3 \cdot 10^{-3}$ and the values of the other parameters in Fig. 1, the time dependence of the center of gravity of the unsettled particles is nearly a straight line. In contrast to the process depicted in Fig. 1, at the indicated value of M the settling is uniform and the upper boundary of the gas suspension is a horizontal straight line. A decrease in M^2 is accompanied by an increase in the frequency of the gas oscillations, so they decay more rapidly. For example, for $M^2 = 3 \cdot 10^{-3}$, the oscillations practically cease within a period of time equal to half the time required for complete settling of the particles.

A change in Re within the investigated range has little effect on the deposition process. An increase in Re corresponds to a reduction in the viscosity of the gas, which means that more momentum is acquired by the carrier phase at the initial stage and that the oscillations which develop decay more slowly. Thus, with $M^2 = 0.05$, $Fr = 40$, and $M_{21} = 0.1$, an increase in Re from 15 to 30 and 60 corresponds to an increase in the maximum total momentum $J(t)$ at the moment $t = t_*$ by about 20% for $Re = 30$ compared to $Re = 15$ and by about 15% for $Re = 60$ compared to $Re = 30$. The curve $y_c(t)$ changes its form only slightly with an increase in Re .

A reduction in the quantity of the disperse phase M_{21} results in a decrease in the momentum imparted to the gas. Accordingly, there is also a decrease in the amplitude of the gas oscillations and their effect on the dynamics of the particles. At $M_{21} \leq 0.01$, the particles settle uniformly in the vessel and the settling process is unidimensional in character.

Figure 3 shows the dynamics of deposition of a gas suspension in the form of the time dependence of the running fraction of settled particles $K(t)$ with $Re = 30$, $Fr = 40$, and $M^2 = 0.05$ and a change in the parameter M_{21} : $M_{21} = 0.5$; 0.2 ; 0.1 ; 0.001 (lines 1-4). The gas oscillations which develop intensify settling. The greater the amplitude of the oscillations, dependent on M_{21} , the more the curve $K(t)$ deviates from the straight line corresponding to uniform settling. It is evident from Fig. 3 that the time required for 50% settling of the particles for $M_{21} = 0.5$ is roughly half the time required at $M_{21} = 0.001$.

As already noted, a reduction in M is accompanied by a decrease in the intensity of the oscillations and their effect on particle deposition. At sufficiently small M , the deposition process is uniform and unidimensional. Even in this case, however, by increasing Fr and thus reducing the particle relaxation time, it is always possible to realize a situation whereby the relaxation time is shorter than the acoustic time. If the mass of the particles is sufficiently large ($M_{21} \sim 1$) in this case, then effects similar to those described above will occur. The ratio $t_s/t_r = FrM \sim 1$ determines the region in which gas oscillations affect the settling process.

4. Comparison with Unidimensional Settling. To study the effect of non-unidimensional phenomena on gas oscillation and particle settling, we calculated the corresponding unidimensional processes. The unidimensional equations were integrated by means of the explicit scheme in [11] on a uniform grid with 21 nodes. The Courant number $Ku = 0.05$.

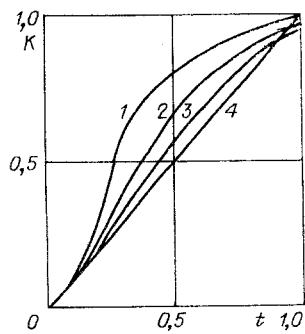


Fig. 3

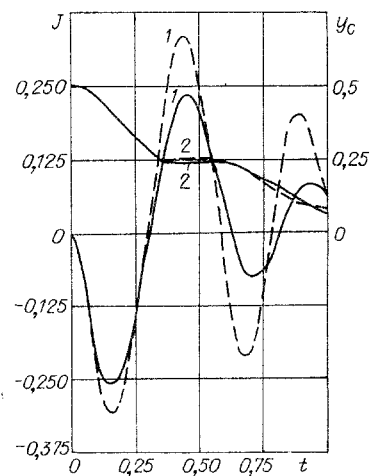


Fig. 4

Relative to the unidimensional case, in the two-dimensional case friction against the side walls of the vessel results in lower acceleration of the gas at the initial (accelerating) stage of motion and faster decay of the oscillations which develop. This in turn leads to more uniform particle settling. Figure 4 shows the total momentum of the gas $J(t)$ and the coordinate of the center of gravity of the unsettled particles $y_c(t)$ (curves 1 and 2) for the unidimensional (dashed lines) and two-dimensional (solid lines) cases with $M^2 = 0.05$, $Re = 30$, $M_{21} = 0.5$, and $Fr = 20$. Within the range of parameters in which gas oscillations are significant, there is a 15-25% relative increase in momentum $J(t)$ in the unidimensional case compared to the two-dimensional case at the moment $t = t_*$.

Thus, the above study shows that, under certain conditions, the hindered settling of a gas suspension is accompanied by gasdynamic oscillations of the carrier phase, these oscillations having a significant effect on the settling process. The gas moves alternately up and down, accelerating or slowing particle settling accordingly. The result of these processes is an intensification of particle deposition. This effect is seen in both unidimensional and two-dimensional cases, but it is less pronounced in the latter case due to friction of the gas against the side walls of the vessel. The method used here to describe the motion of the disperse phase was shown to be highly effective in modeling the motion of a gas suspension with a definite disperse-phase boundary.

LITERATURE CITED

1. H. Hasimoto, "On the periodic fundamental solutions of the Stokes equations and their application to viscous flow past a cubic array of spheres," *J. Fluid Mech.*, **5**, No. 2 (1959).
2. J. Batchelor, "Settling of spherical particles in a low-concentration suspension," *Mekhanika*, No. 4 (1973).
3. V. V. Struminskii, O. B. Gus'kov, and Yu. N. Kul'bitskii, "Hydrodynamics of dispersed and gas-liquid flows," *Dokl. Akad. Nauk SSSR*, **278**, No. 1 (1984).
4. S. Sau, *Hydrodynamics of Multiphase Systems* [Russian translation], Mir, Moscow (1971).
5. W. D. Hill, R. R. Rothfus, and Li Kun, "Boundary-enhanced sedimentation due to settling convection," *Int. J. Multiphase Flow*, **6**, No. 6 (1977).
6. E. Smek, "Two-dimensional viscous flow of a vertical vessel," *Acta Mech.*, **55**, Nos. 1-2 (1985).
7. R. I. Nigmatulin, *Principles of the Mechanics of Heterogeneous Media* [in Russian], Nauka, Moscow (1978).
8. G. M. Makhviladze, O. I. Melikhov, and E. B. Soboleva, "Calculation of flows of gas suspensions in closed volumes," *Chemical Physics of Combustion and Explosion. Kinetics and Combustion: Materials of the VIII All-Union Symposium on Combustion and Explosion*, OIKhF Akad. Nauk SSSR, Chernogolovka (1986).
9. G. M. Makhviladze and S. B. Shcherback, "Numerical method of studying nonsteady three-dimensional motions of a compressible gas," *Inzh. Fiz. Zh.*, **38**, No. 3 (1980).
10. G. M. Makhviladze and O. I. Melikhov, "Motion of a collection of particles under the influence of gravity and its settling on a flat horizontal surface," *Izv. Akad. Nauk SSSR Mekh. Zhidk. Gaza*, No. 6 (1982).

11. I. Yu. Brailovskaya, "Explicit difference methods for calculating open flows of a viscous compressible gas," in: Some Applications of the Grid Method in Gasdynamics [in Russian], Vol. 4, Izd. MGU, Moscow (1971).

PROPAGATION OF NONLINEAR LONGITUDINAL WAVES IN POROUS SATURATED MEDIA

A. M. Ionov, V. K. Sirotkin, and E. V. Sumin

UDC 534.222

A considerable number of works have been devoted to aspects of low-amplitude wave propagation in saturated porous media. A detailed bibliography of studies on this question is given in [1]. As experiments show, the upper layer of the earth's core is characterized by anomalously high values of the nonlinearity parameter [2, 3]. In view of this there is interest in questions connected with studying the propagation of finite-amplitude waves in porous media also exhibiting dispersion-dissipative properties. Nonlinear waves in a Rakhmatullin model (model of equal phase pressures) were considered in [4]. However, it is applicable to a very limited class of geological materials.

In this work a second approximation equation (KdVB) has been obtained describing propagation of longitudinal waves of finite amplitude in saturated porous media. In contrast to [4], in the model in question equality was assumed for pressure in the solid and liquid phases. Analysis of the effect of strength properties for the matrix and impregnating component on the nonlinear dissipative properties of the medium was carried out both for weakly cemented (sands) and for strongly cemented (andesite, granite) materials. Within the suggested model it is possible to describe the anomalously high values of nonlinearity parameter observed by experiment.

1. Continuity and pulse equations for the solid and liquid phases for unidimensional planar movement of a water-saturated medium have the form [1, 5]

$$\begin{aligned} \frac{\partial}{\partial t} (1-m) \rho_1 + \frac{\partial}{\partial x} (1-m) \rho_1 u_1 &= 0, \quad \frac{\partial}{\partial t} m \rho_2 + \frac{\partial}{\partial x} m \rho_2 u_2 = 0, \\ (1-m) \rho_1 \left(\frac{\partial u_1}{\partial t} + u_1 \frac{\partial u_1}{\partial x} \right) &= - \frac{\partial p_{\text{eff}}}{\partial x} + \frac{4}{3} \frac{\partial \tau_{\text{eff}}}{\partial x} - \\ - (1-m) \frac{\partial p_2}{\partial x} + R + (1-m) \rho_1 g, \quad m \rho_2 \left(\frac{\partial u_2}{\partial t} + u_2 \frac{\partial u_2}{\partial x} \right) &= - m \frac{\partial p_2}{\partial x} - R + m \rho_2 g, \end{aligned} \quad (1.1)$$

where ρ_1 , ρ_2 , and u_1 , u_2 are solid and liquid phase density and velocity, respectively; m is medium porosity; p_2 is pore pressure; p_{eff} and τ_{eff} are effective pressure and tangential stress in the medium. Effective pressure p_{eff} is determined by the difference between pressure in the medium $p = (1-m)p_1 + mp_2$ (p_1 is pressure in the solid phase) and pore pressure p_2 :

$$p_{\text{eff}} = p - p_2 = (1-m)(p_1 - p_2). \quad (1.2)$$

We consider the deformation properties of a porous medium saturated with liquid. We shall assume that the difference in current porosity from porosity in the unloaded state is entirely connected with contact compressibility of particles. Whence it follows that porosity only depends on the difference of pressures in the solid phase and in the liquid saturating the pores, and there is a clear correlation between m and p_{eff} :

$$m = m(p_{\text{eff}}). \quad (1.8)$$

For dry rock $p_{\text{eff}} = p$. Therefore, the rule for the change in porosity due to effective pressure (1.3) may be determined from data for the dependence of dry rock compressibility on pressure.